6-2011

SAE Aero Design Project

Angela N. McLelland
Union College - Schenectady, NY

SAE Aero Design Project

Angela McLelland

MER 498-Senior Project

Final Report

March 18, 2011

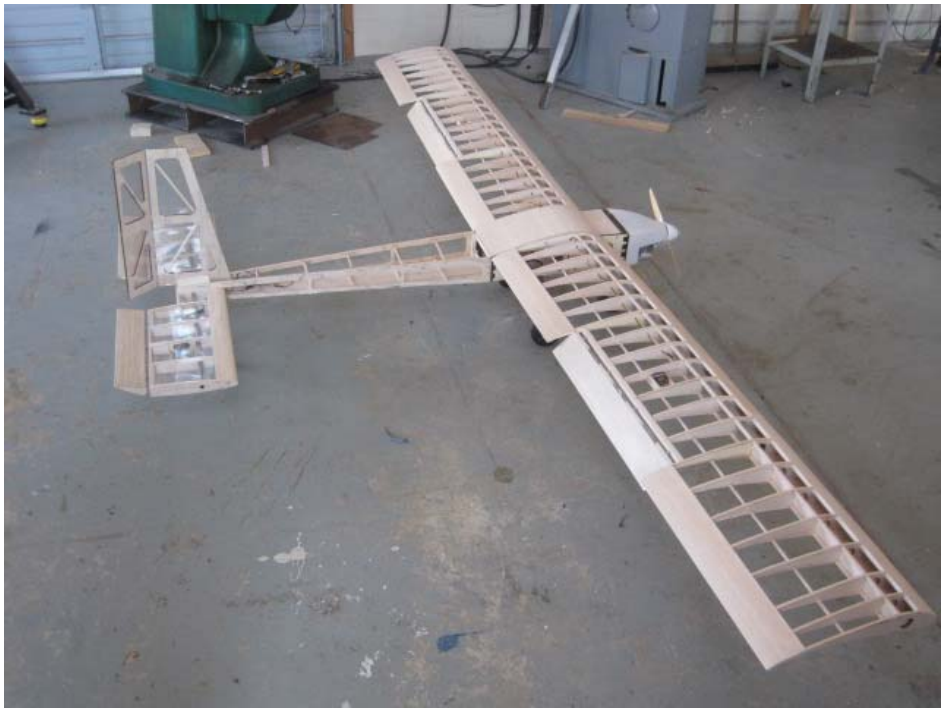

Union College

Schenectady, NY

Department of Mechanical Engineering

Foreword

The Union College Flying Dutchmen Team aims to compete in the spring 2011, SAE Aero Design® East Competition. This regional event, hosted by the Society of Automotive Engineers International, is a threefold opportunity for teams from around the globe to showcase their understanding of engineering fundamentals. Competing in the SAE Aero Design® competition creates an arena for students to participate in hands-on design, to emphasize technological innovations in a competition setting, and to cooperate in a unique atmosphere where intellectual advancement and teamwork are championed above success.

The underlying goal of the SAE Aero Design® competition is to design and construct a high lift plane, capable of carrying upwards of fifty-five pounds. In order to achieve this objective, the 2011 Flying Dutchmen aimed to design a plane with structural integrity, positive static stability and high lift generating aerodynamics. Furthermore, the team took extensive measures to minimize the overall weight of the aircraft yet maintain the critical structural strength required to lift such a payload. In addition to these characteristics, the Flying Dutchmen utilized the design requirements of the competition in order to ensure safety and regulation compliance with power and size constraints.

This year's Flying Dutchmen Team, consisted of three senior mechanical engineering students. Andrew Heitmann, Timothy McGovern, and I each had a specific and fully defined responsibly prior to construction and maintained individual analytical specialties throughout the design process. In order to optimize the strength to weight ratio, the team completed extensive technical investigations in the areas of aerodynamics, structural integrity, and aircraft stability. While sufficient data existed to analyze full-scale airplanes, there were several considerable differences that needed to be considered before designing a radio controlled (R/C) model plane.

Due to the in depth nature of the research and the testing required to design an R/C plane, the Union College Aero team has dedicated two trimesters (approximately 25 weeks) and a considerable senior project budget to constructing the most successful plane possible. In order to ensure sound engineering design decision, Professors Bradford

Bruno, Ph. D. and Ashok Ramasubramanian, Ph.D., this year's senior project advisors, requested that the Abaqus and ANSYS software packages be utilized. These computer aided tools aided in addressing the following design questions:

Wing and Tail Design

1.) What airfoil(s) has the highest coefficient of lift and is it feasible for construction?
2.) What wing configuration and aspect ratio offers the most stability?
3.) What is the maximum wing loading at any position during flight?
4.) How can the weight/strength ratio be optimized through design and material selection?
5.) What quantitative counter moment, must the tail produce, in order to correct the nose heavy tendency created by the weight of the motor?

Fuselage and Landing Gear Design

1.) What fuselage design allows for secure positioning of the payload over the center of gravity yet minimizes frontal area?
2.) What wing/fuselage, landing gear/fuselage and tail/fuselage interfaces are most structurally secure?
3.) What loads will the landing gear experience during landing?

The purpose of this report will be to technically justify the current wing design of The Flying Dutchmen's plane and provide useful, computational analysis to aid in the design of future Union College Aero teams. Furthermore, a brief description of the 2011 Flying Dutchmen plane will be discussed as well as a few of the specific design trade-offs that contributed to the proposed design.

Executive Summary

Purpose and Methodology

The objective of this project is to design a high lift, R/C plane capable of carrying a maximum payload of fifty-five pounds in competition. More specifically, the independent project objective of this senior project was to design an aerodynamically efficient plane that optimizes the useful lifting area of a wing while minimizing its induced drag. The main focus of the first term was to produce a robust design with construction feasibility and the capacity for modifications after full scale testing has been completed. This goal was achieved by completing 3D, Computational Fluid Dynamics (CFD) simulation in order to confirm online airfoil data. The second term of the project allowed for scaled wind tunnel testing of the full plane as well as full scale construction.

Test Results

As a result of external investigations and the conclusive data obtained through CFD simulations, the airfoil chosen for this year's plane was the Selig 1223. In order to remain within the size envelope set by competition regulations yet maximize wing area, the wing was designed to be 14x120 inches. With a maximum lift coefficient of 2.425, ideally this airfoil could produce approximately 200 N of lift force at an air speed of 25 mph. CFD demonstrated that while some lifting ability is lost, due to the non-infinite surface of the three dimensional wing, the actual coefficient of the wing was within 5% of the published data. Wind tunnel testing of a $1/12^{th}$ model later provided a realistic indication of the full planes lift capabilities.

In accordance with competition requirements, a performance analysis of the plane was completed in order to generate a payload prediction graph. The results of this analysis verify both the computational and experimental aerodynamic results and suggest that, at sea level, the plane will be able to take-off successfully with a payload of 24.9lbs. This value was considered satisfactory for competition success and should define the engineering success of the proposed design.

Table of Contents

List of Figures and Tables

Figures

Tables and Charts

1 Introduction

1.1 Organizational Context

Every year, The Society of Automotive Engineers (SAE), hosts two nationwide airplane design competitions. These competitions challenge teams from around the globe to design and build radio controlled (R/C) model airplanes. Constricted by the power class of the engine and an established size constraint, these planes are judged primarily on the maximum gross weight lifted. The competition changes location yearly, with the most recent being held in Forth Worth, Texas, and this year's in Marietta, Georgia. Along with the flight and physical competition, a high percentage of the ranking relies on an oral presentation and extensive design report. The competition features three classes: Regular, Advanced, and Micro. The 2011 Flying Dutchmen have entered the Regular Class Division, which is intended to be the most accessible class.

This regional event is a three-fold opportunity for any student committed enough to attempt the challenge. First and foremost, competing in the SAE Aero design competition presents a real-life, hands-on and fast pace dimension to the Engineering curriculum presented here at Union College. Secondly, the SAE Aero Competition presents an opportunity for students to represent university engineering in a competitive setting. Lastly, the SAE Aero design competition offers a unique and cooperative atmosphere; which, with the collaboration of various sponsors, promises to highlight the best Union has to offer. While past Union teams have preformed quite admirably this year's goal is to rank higher than ever before, an attainable goal considering the team consists of three senior mechanical engineering students.

1.2 Project Objectives

To obtain senior project credit and successful competition participation, the Flying Dutchmen team decided to design and build a plane with the following three criteria: structural integrity, positive static stability and high lift generating aerodynamics. Personal concentration was concerned on analyzing the aerodynamics of the chosen wing, optimizing the fuselage final design to reduce frontal area and researching various tail configurations to correct the nose down tendency inherent to the plane. The

guidelines followed throughout the design of the plane were specified by SAE completion rules. More specifically, for the 2011 competition:

- No lighter-than air or rotary wing aircraft such as helicopters or autogyros will be allowed to compete.
- Fully configured for takeoff, the freestanding aircraft shall have a maximum combined length, width, and height of 225 inches.
- Regular Class aircraft may not weigh more than fifty-five (55) pounds with payload and fuel.
- Must be capable of carrying a fully enclosed single payload.

[1]

Ultimately, this year's Flying Dutchmen sought to scientifically support the proposed design decisions with various software packages, network with flying enthusiasts to establish reliable resources for future teams, tests various prototypes, and construct a competitive airplane capable of taking home the gold.

1.3 Report Layout

This report will first discuss the previous efforts made by Union College teams and their successes at past SAE Aero Competitions. Next, a functional decomposition of the plane along with various plane configurations and design options will be discussed. This overview will be followed by a brief literature review analyzing the advancements made in the studies of model plane aerodynamics and the principles of flight which motivated this research. These principles lead directly into a discussion of airfoil selection and the various numerical analyses that such comparisons can provide. After relevant background information has been presented, a brief description of the current wing design, including airfoil selection, design specifications, and correction factors, will be justified. The analysis utilized to reach the current design and a brief conclusion of the team's construction feasibility research will conclude the design aspect of this progress report. Lastly, the team's final plane design will be discussed as well as a brief overview of 'non-project specific' achievements.

2 Background

The Flying Dutchmen utilized a variety of intellectual resources in the primary investigation of Remote Controlled (R/C) plane design. Such resources included a literary review of pertinent published works, design reviews of previous Union College teams, and emphatic tests. The results of this preliminary research are summarized below.

2.1 Flying Dutchmen of the Past

Over the past five years, the Mechanical Engineering Department at Union has sponsored four SAE Aero Design projects. The teams from 2009 and 2010 both built fully functioning planes and entered into the competition. In 2009 the team placed twenty-first overall, while the 2010 team placed thirty-fourth overall. Both of these results are respectable considering the 2009 team was Union's first official entry and the 2010 team consisted of sophomores lacking some of the essential coursework for airplane design. These four teams, specifically the past two, have produced solid base reports and design documentation for the groundwork of this project. The efforts of this year's team will generate Union's initial database of analytical resources and test results to better equip future teams for success.

2.2 Tests and Equipment

The 2011 Flying Dutchmen design process relied heavily on a series of built-in 'sanity checks.' These emphatic tests were utilized to gauge the validity of numeric calculations and qualify the literary research. For example, in the early stages of research a test apparatus was constructed to measure the engine's trust production. The results of this test impacted lift calculations, which eventually dictated the planform area and overall dimensions of the plane. Likewise, simplified wing models were subjected to weight bearing tests to ensure that the spar design would be adequate for the desired payload. While these test were not considered advance engineering analyses, the results proved to be invaluable to the final design of the plane. Moreover, the tests saved valuable time during the latter phase of the project by providing an accurate estimate of supply delivery timeframes and wing construction time demands.

2.3 Functional Decomposition

There are six main functional categories that require design, analysis, and testing prior to successful flight. These six groupings each play a vital role in one of the three main objectives set in order to achieve competition success: aerodynamics, stability, and structural integrity. While the functional classifications may ultimately overlap, each plane component serves to achieve a specific and unique goal. The power plant of the plane consists of the motor, propeller, and fuel utilized to generate energy for the plane. While these criteria are specified by competition standards, the placement of these components in relation to other plane parts, their spatial configuration as it affects the center of gravity, and the mounting mechanisms utilized to secure the plant to the plane, will all directly impact the aforementioned project goals respectively. The control surfaces such as ailerons, rudder, and elevator will play a vital role in the neutrality of flight as well as pilot input control. Such factors will clearly dictate the handling characteristics of the plane and thus the plane's stability during flight. The wing of the airplane will generate the majority of lift, a fundamental aerodynamic force governing flight. The tail of the wing will serve to counter balance the moment created by the weight of the power plant and pitch of the wing. This feature of the plane will require both aerodynamic shaping to minimize drag as well as correct placement to ensure lateral stability of the plane. The plane's landing gear will be used to direct the nose of the plane during take-off taxiing and will need to bear the full weight of the plane, and its momentum, during landing. This sub-mechanism of the plane therefore requires optimization between strength and size and creates a great opportunity to cut the plane's overall gross weight. The fuselage of the plane will house the payload and serve as the central point of connection for the rest of the plane. These interfaces present significant structural weakness and will need to be analyzed in order to ensure in-flight forces will not exceed the material durability.

For each of these functional micro-systems, there are several workable design options. The effectiveness of a plane's control surface, for instance, is proportional to the total surface area of the feature. One example of this is in the design of aileron size. This aileron surface area is expressed as a total percentage of the stab span is based on wing area, which is attached to the plane in some range of the fuselage length and so on. These

design decisions primarily affect the stability of the plane and are further discussed in Andrew Heitmann's paper. Wing placement is another design aspect where several interface options each offer a multitude of flight behaviors. Such attachment options include high wing, bi-plane, low wing and mid wing options. Lastly, there are two unique landing gear configurations that can be considered. Tail draggers and tricycle landing gears each have specific pros and cons and will be fully analyzed by Timothy McGovern in his final design report.

2.4 Aerodynamic Fundamentals

2.4.1 Lift

Flight is a delicate balancing act between four primary forces. While in flight, an airplane body is subjected to lift, drag, thrust and weight. Only when these four forces are in equilibrium can level, steady flight be achieved. Lift, is the force that acts through the body of an aircraft and directly opposes its weight. More specifically, lift is the component of the aerodynamic force exerted by the air on an airfoil, having a direction perpendicular to the direction of motion and causing an aircraft to stay aloft [2]. Lift can be expressed by the following equation:

$$L = \frac{\rho * v^2 * A * C_L}{2}$$

Equation 1

*Where L is the lifting force measured in Newtons, ρ is the density of air, v is the velocity of the plane, A is the wing's total planform area, and C_L is the coefficient of lift associated with the airfoil.

As the above equation suggests, there are three ways to increase the lifting force of a plane: an alteration of the airfoil selection (which determines the max coefficient of lift), an increase in the plane's relative air speed, or an increase in the total lift producing area. While the wings of an airplane are the largest generators of lift, the total lifting force is actually impacted by several physical components. Such components include the tail and fuselage of the plane; however, the contributions made by such parts are nominal and can be disregarded in the initial lift calculations of plane design.

2.4.2 Drag:

The force that impedes forward progression of a plane through the air is known as drag. A plane's total drag can be clearly divided into two main categories: induced drag and parasitic drag. Induced drag is the result of a wing's lift generation. In other words, lift cannot be generated without some amount of induced drag being produced. This symbiotic relationship is due to the Bernoulli Principle. Simply stated, Bernoulli's Principle expresses that as the velocity of air over a given area increases, its exerted pressure decreases. Thus, as the shape of an airfoil accelerates air over the top of a wing, pressure is lowered simultaneously, and the counter reaction occurs on the underside. As a result of this imbalance in pressure, and in an attempt to establish equilibrium, high-pressure air moves outward along the wing and curls up at the tip as well as downward over the top. This latter motion results in a down force directly following the trailing edge. These two reactions are called wing tip vortices and downwash, respectively. Downwash is essentially the cause of induced drag.

Unlike induced drag, parasitic drag directly hinders the forward motion of an aircraft and is unrelated to any positive lift generation. The three types of parasitic drag are form, interference, and skin drag. Form drag is a result of the aerodynamic shape of plane components such as the fuselage, wings, tail, landing gear, and propeller. Interference drag is a consequence of turbulence formed in airflow as a result of sharp edges or perpendicular interfaces of plane components. Lastly, skin drag is a product of small imperfections on surfaces such as wrinkles or dimples [3].

The overall drag of the plane is a summation of both induced and parasitic drag and can be expressed by the following equation:

$$D=\frac{\rho * v^2 * A * C_D}{2}$$

Equation 2

*Where D is the drag force measured in Newtons, ρ is the density of air, v is the velocity of the plane, A is the total surface area of the plane and C_D is the plane's coefficient of drag.

3 Wing Design

3.1 Airfoil Selection

Undoubtedly, airfoil selection is the most influential decision impacting wing lift generation. There are several airfoil characteristics that contribute to overall wing performance and flight behaviors. For example, the stalling pattern of the airfoil determines the rate at which lift drops off after maximum performance is achieved. These patterns are classified as sharp, sudden, or gentle and determine how the wing will fail at the instant of over ascent. Another important characteristic of an airfoil is the mean camber line. Camber is the maximum distance measured between the chord (straight line drawn between leading and trailing edge) and mean camber line (center line of airfoil profile.) Increase camber produces higher maximum lift coefficients and produces lift at larger, negative angles of attack values [4].

The three main characteristics, unique to any airfoil, the coefficient of lift (C_L), coefficient of drag (C_D), and the pitching moment (C_M) vary as a result of the Angle of Attack (AoA.) The values for these coefficients are not only dependent on the airfoil selection but also on the velocity, or more specifically, the Reynolds Number at which the plane will be operating. This non-dimensional number serves as a scaling factor and is represented below:

$$\mathrm{Re} = \frac{\rho v L}{\mu}$$

Equation 3

*Where Re is the Reynolds Number, ρ is the density of air, v is the velocity of the plane, L is the characteristic length of the wing (i.e. chord length), and μ in the air's viscosity.

These coefficients along with six other three dimensional design parameters determine the values for lift and drag. These parameters are: speed, wing chord, planform, wing area, angle of attack, and aspect ratio and must be evaluated as primary design decisions. The evaluation of these parameters relies on rigorous optimization of design specifications as well as external research to supplement the team's analysis.

3.2 Final Airfoil Selection

The Flying Dutchmen Team 2011 has decided to utilize the Selig 1223. The physical characteristics of this airfoil are the most advantageous for the heavy lift aspect of the competition.

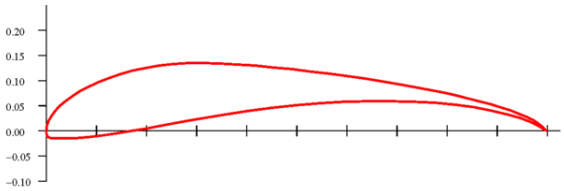

***Figure 1*:** S1223 Airfoil Profile

Profile of the S1223 Airfoil: this curve can be scaled to incorporate design specifications such as chord and main spar size [5].

***Chart 1*:** S1223 Lift Characteristics

Lift and pitching moment coefficients at various angles of attack for the S1223 [5]

As can be seen above, in *Figure 1*, S1223 is a highly cambered airfoil with a low thickness and relatively slender trailing edge. These physical traits lend to sudden lift loss at the stall angle of attack, as seen in *Chart 1*, and can be expressed numerically by the values in *Table 1*.

Camber:	Max C_L:	Max C_L angle:	Max L/D:	Max L/D angle:	Max L/D C_L:	Stall angle:	Zero-lift angle:
8.70%	2.425	8	71.86	5.5	2.185	8	-13

Table 1: S1223 Airfoil Characteristics

Table 1 offers numerical values for various lift features depicted in Chart1. From the absolute value between stall angle and zero-lift angle modelers can determine workable mounting angles as well as aerobatic properties, or in this case, the lack there of. [5]

3.3 Specifications

Wing design required the optimization of weight, area, strength, and competition regulations. Given the summation of length, width, and height constraint set for the overall plane design (i.e. that the span + plane length + plane height ≤ 225 inches), the notion that the plane length should be between 60-80% of wing span, and a safety envelope of ten inches, the following formulas were utilized to determine a feasible range of wing spans:

$$10+S+L+H \leq 225$$

Equation 4

*Where S is the wingspan, L in the plane's length, and H is the plane's height.

Equation 4 is a modified version of the equation utilized by competition officials to quantify the size of a plane. This modification includes the teams' built-in cushion of ten inches. This safety allows for slight alterations of the fuselage length as well as protects against unforeseen obstacles during construction. Below, *Equation 5*, demonstrates basic modeling convention rages for the length of plane with respect to the span of a wing.

$$.8*S \leq L \leq .6*S$$

Equation 5

These equations yielded a feasibility range for the wingspan dimension. Next, the required lift force needed to hold the maximum payload was determined. This was achieved by utilizing a free body diagram of a plane in steady level flight.

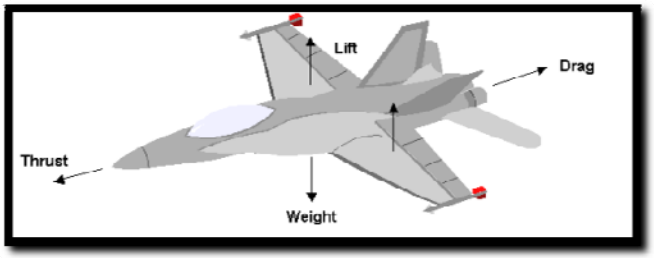

Figure 2: Free Body Diagram of Forces in Flight [6]

As can be seen, lift acts over the entire surface of the wing while weigh is concentrated load acting through the center of gravity

In this particular state, the plane's lift force is equal and opposite the total net weight of the aircraft. Thus, if the Flying Dutchmen plane was to succeed in lifting the maximum gross weight of fifty-five pounds, the total lifting force required would be approximately 245N. This value was then substituted into *Equation 1*, along with the Max C_L of the airfoil (see *Table 1*) and evaluated to determine what chord lengths could realistically generate the required lift; while, maintaining sensible velocities, a factor dependent on the power plant of the plane. A sample spreadsheet of this optimization for the chosen chord length is shown below in *Table 2*. Other chord lengths were eliminated due to the high velocities required to generate the needed lift. For the available thrust of the plane, a viable velocity range was determined to be between the zero and thirty miles per hour.

Chord- 14					
Velocity (mph)	Lift (100)	Lift (110)	Lift (120)	Lift (130)	Lift (140)
0	0.00	0.00	0.00	0.00	0.00
5	6.59	7.25	7.91	8.56	9.22
10	26.35	28.99	31.62	34.26	36.89
15	59.29	65.22	71.15	77.08	83.01
20	105.41	115.95	126.50	137.04	147.58
25	164.71	181.18	197.65	214.12	230.59
30	237.18	260.90	284.61	308.33	332.05
35	322.83	355.11	387.39	419.67	451.96
40	421.65	463.82	505.98	548.15	590.31
45	533.65	587.02	640.38	693.75	747.11
50	658.83	724.71	790.59	856.48	922.36

***Table 2**:* Lifting Force Generated

The table above, shows the lift generated by various spans and at various velocities for a fourteen-inch chord wing. The values that lie on either side of the required lifting load have been highlighted.

These values were then cross referenced with another important design specification, a wing's aspect ratio. Aspect Ratio is defined as the ratio of a wing's span

to chord. This value quantifies the slenderness or stoutness of a wing and determines what type of gliding behaviors the wing will exhibit.

$$AR = \frac{s^2}{A}$$

Equation 6

Wings with "high aspect ratios have long spans (like high performance gliders), while low aspect ratio wings have either short spans or thick chords (like the Space Shuttle). Gliders have a high aspect ratio because the drag of the aircraft depends on this parameter. A higher aspect ratio gives a lower drag, a higher lift to drag ratio, and a better glide angle [7]." Thus, this year's Flying Dutchmen wanted a wing with an aspect ratio between seven and ten. The table below evaluated the results of *Equations 4-6* to determine viable wing configurations.

Chord (inches)	**Aspect Ratio (100)**	**Aspect Ratio (110)**	**Aspect Ratio (120)**	**Aspect Ratio (130)**	**Aspect Ratio (140)**
9	11.11	12.22	13.33	14.44	15.56
10	10.00	11.00	12.00	13.00	14.00
11	9.09	10.00	10.91	11.82	12.73
12	8.33	9.17	10.00	10.83	11.67
13	7.69	8.46	9.23	10.00	10.77
14	7.14	7.86	8.57	9.29	10.00
15	6.67	7.33	8.00	8.67	9.33
16	6.25	6.88	7.50	8.13	8.75

Table 3: Aspect Ratio for Various Wing Configurations

The table to the left shows the aspect ratio of various chords and spans (shown in parenthesis across the top row.) Aspect ratios that fall in the working range are highlighted in green.

After a chord of fourteen inches and a span of one hundred and twenty inches were chosen (*see Figure 3 for CAD model*), the final wing parameter that had to be determined was the planform area. Planform is the area of the wing, as seen from above.

Since the root, near the plane, and tip chord are equal, the planform area of this year's Flying Dutchmen team is rectangular. That is, the top down view of the wing is rectangular and will not perform as the more efficient elliptical wing.

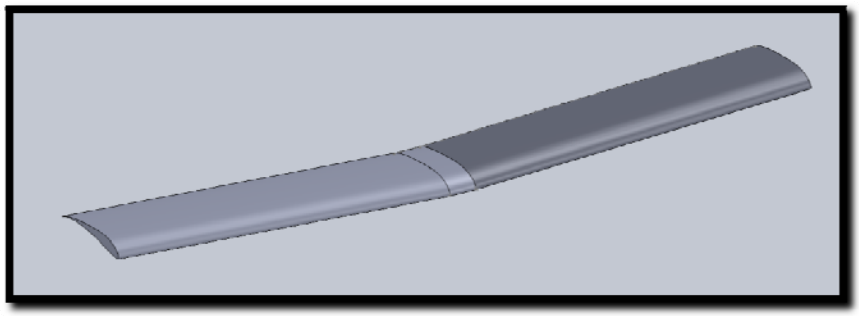

Figure 3: 2010 Flying Dutchmen Wing, SolidWorks Rendering

Shown above is the 3D CAD model of this year's wing design.

3.4 Stability and Strength

In order to ensure that the plane naturally resumes straight and level flight after a slight input to the controller has been made, dihedral was built into the plane. Dihedral is defined as the upward slope of an airplane's wing [8]. Shown below, this angle of incline does not require an extreme value and is actually most efficient between two and five degrees. The dihedral of the Dutchmen plane was constructed to be 5°.

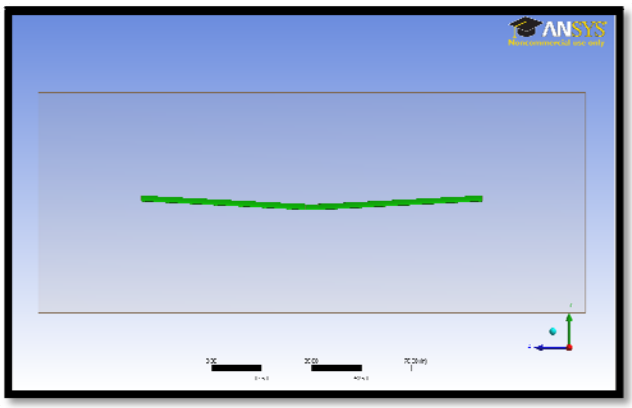

Figure 4: 2010 Flying Dutchmen Wing

Above, a dihedral of three degrees can be seen on over both the left and right segments of wing.

Furthermore, washout was incorporated into the final wing design. Wash out is a built-in, purposeful twist in the wing from root to tip. This twisting ensures that as the plane reaches an angle of attack, close to the stall angle, the tip of the wing stalls before the root. Since the aileron position of this year's team is located near the tip, the wash out will be constructed in such a way that the root stalls first. This will allow the tips, and thus the ailerons, to remain effective after the initial stall occurs. The washout for the final plane was design with a 3° rotation from the chord line at the root and is within standard modeling ranges.

While not considered physical control surfaces, the position of the plane's overall center of gravity affects the overall stability of flight. The center of gravity is the effective 'center' of the plane. At the center of gravity, the moments created by the weight of each component balance all mass is effectively reduced to that location. The location of this point, in relation to the dynamic center of lift, is paramount to the plane's stability and was repeatedly calculated throughout the design.

Another vital aspect of wing design is the wing loading. Wing loading determines the load, or weight, per unit area of the wing, Equation 7. This value determines the structural strength needed by the main aluminum spar and its smaller wood counterparts, which run parallel to the leading edge. Based on the wing loading the necessary strength (ultimately a key factor in total weight) can be optimized and designed to operate at maximum efficiency. For more on this analysis, refer to Timothy McGovern's progress report.

3.5 Correction Factors

In order to fully utilize the data given by the airfoils chart, it is important to understand the operational conditions of the airplane. More specifically, will the presence of turbulence affect flow separation as the air passes over the top of the wing? In order to determine this, the Reynolds Number must be calculated. As stated in Equation 3, this non-dimensional number relates relative velocity, fluid viscosity, and density to predict the fluid behavior, which can be found using an acceptable maximum velocity of 25 mph (see *Table 2*) and given the following regional data for Marietta, GA:

- Average Temperature in May: 66.5°F
- Elevation of Marietta, GA: 1128 ft

The Reynolds number for this wing design was determined to be 2.4E5. This value conventionally represents laminar flow and therefore may separate from the wings surface before the trailing edge is reached. This value also dictated the max C_L achievable and the stall angle of the airfoil (*see Chart 1*).

Furthermore, corrections had to be made in order to relate the two dimensional airfoil data, obtained from an infinite model void of end affect, to actual three-dimensional wings. For the 3D wings designed, the effective angle of attack was determined. This value was larger than the idealized geometric angle of attack captured in 2D simulations of the airfoil. This increase in AoA accounted for the aspect ratio and planform area of a wing. The equation that expressed the total angle of attack needed is shown below:

$$a = \frac{a_o + 18.24 * C_L * (1 + \tau)}{AR}$$

Equation 8

**Where a is the total AoA needed, a_o is the AoA expressed on the airfoil plot, C_L is the coefficient of lift at that AoA, τ is the planform adjustment factor , and AR is the aspect ratio of the wing [4].*

Planform shapes also impact the overall drag a wing produces. In order to account for this deviation from experimental data, the following equation was utilized:

$$C_D = \frac{C_{D_0} + .318 * {C_L}^2 * (1 + \sigma)}{AR}$$

Equation 9

**Where C_D is the total profile and induce drag, C_{D_0} is the section profile drag coefficient at the chosen C_L, ${C_L}^2$ is the coefficient of lift 'square', σ is the planform adjustment factor, and AR is the aspect ratio of the wing [4].*

Using *Equation 8* and the, "Straight wing correction factor for non-elliptic lift distribution" graph, The Basics of R/C Model Aircraft Design [4] (Pg. 6), the planform adjustment factor and total angle of attack were found to be .22 and 5.54˚, respectively. This value was later used to validate computational results and quantify the adverse impact end effect has on the overall expected lift of the plane.

4 Analysis Methods

4.1 Computational Fluid Dynamics

In order to test end effects, establish a numerical value for the actual wing's coefficient of lift and determine the relative velocities and pressures of the wing's surface, computation fluid dynamics (CFD) was utilized. To complete this task, ANSYS 12.0- Workbench was employed. Within the program, a six step solution was established and the results were as follows.

4.1.1 Geometry

In order to analyze the wing for the 2010 team, the SolidWorks CAD model was imported in Workbench. Next, a volume of air had to be created which surrounded the wing. In an attempt to eliminate back flow and flow interference, this volume was arranged so that a thirty-six inch cushion surrounded every face of the wing, *see Figure 7*. The volume of air was created using an 'Enclosure' feature which required one smooth body. Due to the multi-body (center wing, right wing, and left wing) design of the wing in SolidWorks however, 'Virtual Topology' was applied. Ultimately, this topology created virtual surfaces over the harsh angle interfaces between the different sections of the wing. Another helpful feature that 'Enclosure' allowed was the use of symmetry conditions. As a result of this wing's symmetry about the center axis, only half of the physical wing needed to be analyzed in Workbench. This reduction of volume increased the number of mesh elements available and ultimately promoted a more accurate result.

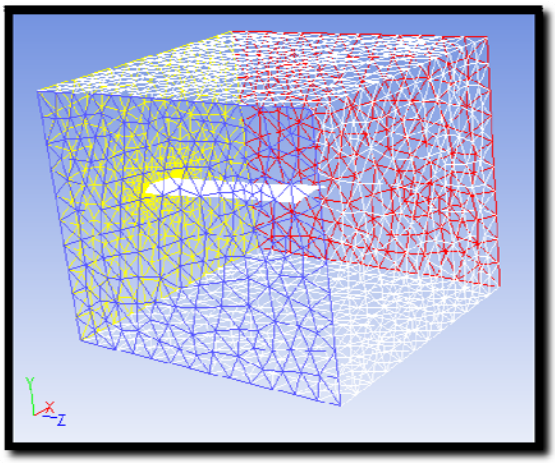

Figure 5: Wing and Enclosure

In the above figure the yellow surface is the symmetry plane of the model, the blue surface is the velocity input, the red surface is the output, and all white surfaces and walls with no-slip condition applied.

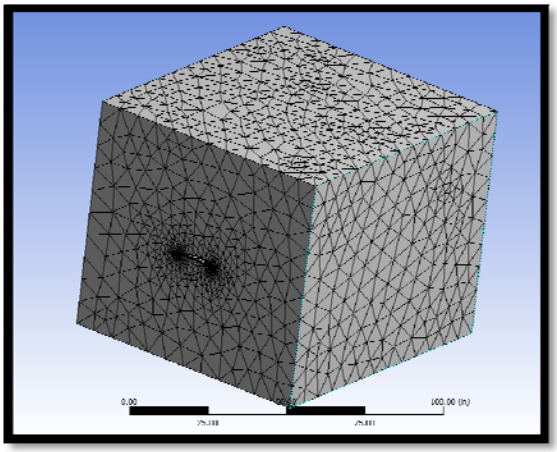

Figure 6: Mesh at Symmetry Plane

Above, the Mesh for the wing is shown. Notice the smaller more refined cells located at areas of his interest, i.e. on the wing surface and more specifically, around the leading and trailing edges.

4.1.2 Mesh

Next, the wing geometry and associated enclosure was imported into the mesh generator and a mesh was produced, *see Figure 6*. In order to produce a viable solution, fine mesh elements had to be created closer to the wing surface and allowed to increase in size exponentially with the distance traveled away from the wing. This 'Growth Rate' helped maintain the overall number of meshing elements and constrained the overall size of the mesh to approximately 512,000 elements. During the meshing process, the inlet, outlet, and other boundary conditions were identified. Finally, the wing body was suppressed; leaving a cavity in the 'enclosure,' and the mesh was created.

4.1.3 Setup

After creating the mesh, boundary conditions were applied. These conditions dictated the physical laws applied to each surface, i.e. The No Slip Condition. Below is a list of those boundary conditions used for the wing's eight surfaces.

Boundaries	
Boundary - bottom_wall	
Type	WALL
Boundary - far_wall	
Type	WALL
Boundary - inlet	
Type	VELOCITY-INLET
Boundary - outlet	
Type	PRESSURE-OUTLET
Boundary - symmetry	
Type	SYMMETRY
Boundary - top_wall	
Type	WALL
Boundary - wall solid	
Type	WALL
Boundary - wing	
Type	WALL

Table 4: Wing Simulation Boundary Physics

This table shows the boundary name, a user defined variable, and the type of physical condition utilized at that boundary.

4.1.4 Solution

After the simulation parameters were adjusted to model the physics of flight, the solution was "Initialized." At this point in the simulation, the number of iterations was specified. In order to ensure grid independence and convergence, the number of iterations was set to 500. This ensured that the smallest amount of 'air' possible was lost during simulation.

During this simulation, the coefficient of lift for the wing was determined to be 1.039 for a 'zero' angle of attack, see *Table 5* below.

Forces - Direction Vector (0 1 0)						
	Forces (n)			Coefficients		
Zone	Pressure	Viscous	Total	Pressure	Viscous	Total
wing	40.347652	0.050548088	40.398201	1.0379366	0.0013003411	1.039237

Table 5: Wing Simulation Results

This table shows the lift forces and coefficients over the wing.

As a result of the correction factor calculations, the actual angle of attack behaves like the geometric angle with a variance of -5.54˚. When this AoA is observed on the airfoil's coefficient of lift graph, Chart1, the C_L value is slightly less than 1.1. Thus, the CFD results confirmed the published data to within 5% of the actual value.

4.1.5 Results

The following images were generated as a result of the ANSYS analysis and show specific flow characterizations. For example, *Figure 7*, shows the wing tip vortices discussed earlier.

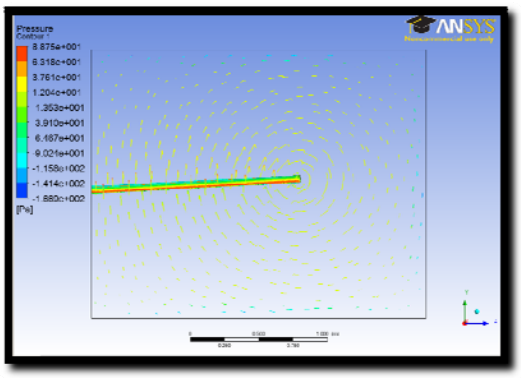

***Figure 7*:** Rear View of Wing and Streamline Field

Above, wing tip vortices are shown from the rear of the wing.

Furthermore, the pressure distribution over the wing was determined and is displayed below. The observed pressure distribution of the simulation confirms the published data regarding the wing loading of a rectangular planform area.

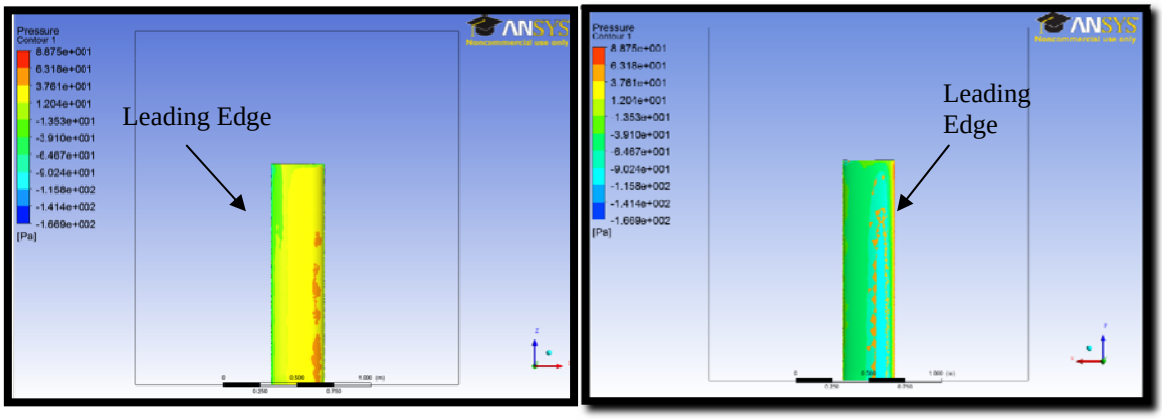

Figure 7: Pressure Distribution

The figure above represents the pressure distribution over the top (left figure) and bottom (right figure) of the wing. The scale shown on each figure represents gauge pressure in Pascals.

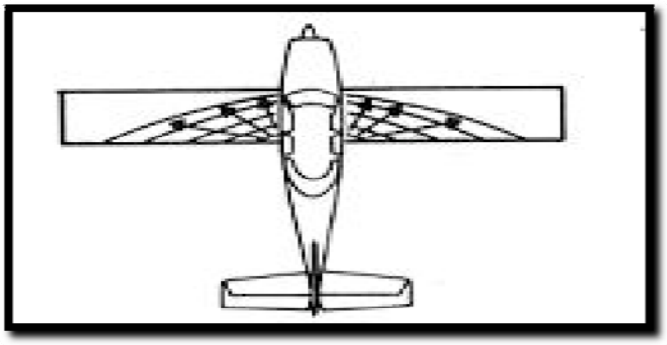

Figure 8: Published Wing Loading

Picture Credit: Lipo Pilot

The above pressure distribution corresponds to the average velocities both over and under the wing. Streamlines around the wing show the relative air speed and the relationship between pressure and velocity can be explained by Bernoulli's Principle. As a simulation 'sanity check,' Bernoulli's Equation was utilized for the applied inlet and

out let velocities. It was thus concluded that the values obtained through ANSYS were an accurate representation of the physical behavior of air for this particular air foil.

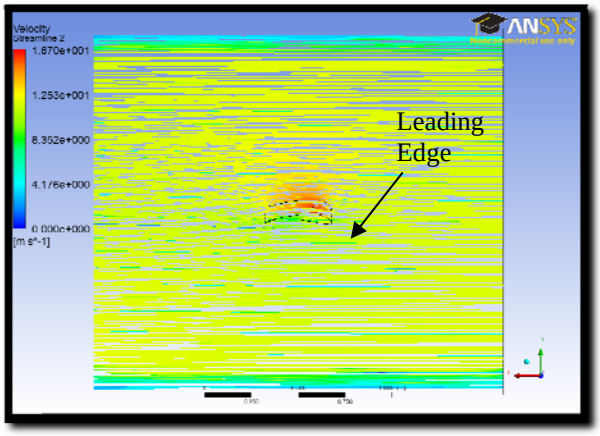

Figure 9: Velocity Profile

The figure above represents the velocity profile around the wing. The scale shown represents velocity in m/s. As can be seen the air travels around 16.7 m/s over the top of the wing. This correlaates to a speed of approximately 37 mph.

4.2 Wind Tunnel Testing

After computational results were obtained, experimental data was utilized to validate the effectiveness of the simulation. Initially, the method for this test was to consider the lift and drag of a single wing. While the construction for this test was completed during the first term of research, see *Appendix A*, and thus would take little time to execute, it was determined that the results would be difficult to correlate to the entire plane. Due to the fact that several of the individual bodies on the plane generate a positive lift, establishing the coefficient of lift for only the wing would be a poor indicator of the plane's actual lifting capacity. As a solution to this problem, the original testing apparatus was revised and the entire plane was modeled to fit inside the wind tunnel.

In order to test a 'scaled' model of the plane, several factors were considered. First, a Buckingham Pi Theorem analysis was completed in order to determine which non-dimensionalized ratios were required to maintain dynamic similarity. To ensure that all relevant the pi groups were established, the variable and units affecting lift were listed, see Table 6.

Variable	Description	Dimensions
F_L	lift force	$M(L)(t^{-2})$
V	velocity	$L(t^{-1})$
L_C	chord length	L
ρ	density	$M(L^{-3})$
μ	viscosity	$M(L^{-1})(t^{-1})$
α	angle of attack	Dimensionless

Table 6: Factors Affecting Lift and Relevant Units

The table above shows the factors of lift and the units of each factor in basic form. That is, M represents mass, L represent length, and t indicates a unit of time. The highlighted factors were utilized and the repeating variables for this analysis.

After repeating variables were chosen and the exponents of each variable were equated to ensure a unitless outcome, the coefficient of lift was determined to be dependent on Reynolds number and angle of attack, see *Equation 10*.

$$\frac{F_L}{\rho V^2 {L_C}^2} = f\left(\frac{\rho\, v\, L_C}{\mu}, \alpha\right)$$

Equation 10

Next, a model of the plane had to be constructed. Due to limited space in the test section of the wind tunnel, a $1/12^{th}$ model was utilized, *Figure 8*.

***Figure 10*:** $1/12^{th}$ Model

The above figure shows the wind tunnel testing model, mounted to the dynamometer shaft.

This sizing of the model allowed for one inch of clearance on either side of the plane's wing. The model plane was constructed using the rapid prototype machine. The material of the rapid prototype was initially included in the team's budget and did not require any additional funding. One obstacle this material created, however, was that the resolution of the printer was not small enough to ensure relative roughness similarity between the model and actual plane. Due to the comparative size of the model, the otherwise small imperfections, caused by the rapid prototype machine's curing process, drastically altered the drag coefficient of the test subject. To compensate for the overly rough surface, the fuselage of the model was coated in modeling clay and the wings and tail pieces were sanded with a varying grade sand paper.

Finally the plane was mounted to the dynamometer and the wind tunnel test was conducted to find the total lift and drag of the plane, see below.

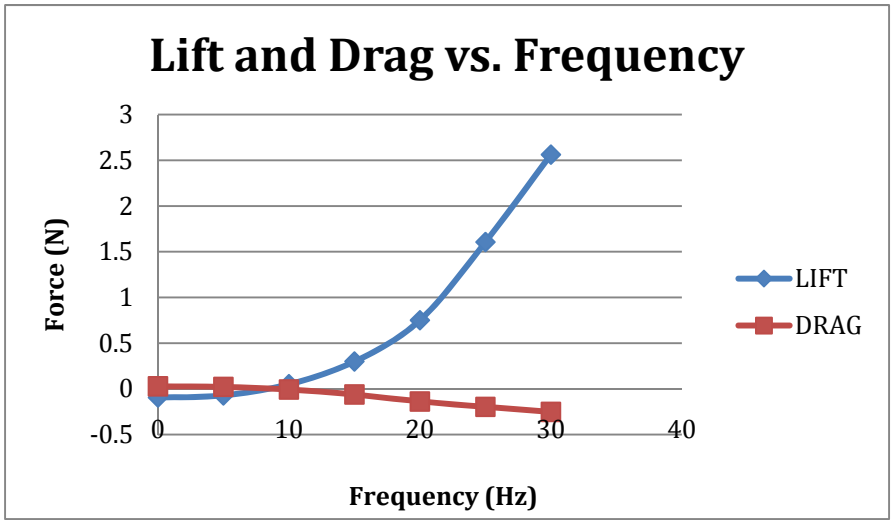

Figure 11: Lift and Drag Data for 1/12th Model

The above figure shows how the lift and drag of the model plane changed at different frequencies. Note: The wind tunnel was not run at full capacity to ensure that the model remained intact.

The frequencies of the wind tunnel were later correlated to velocities, using Pitot tube measurements. The coefficient of lift, calculated for the three dimensional wing with

the CFD simulation, was then utilized to compare the lift force of the model to the potential lifting force of the full sized plane. The results of the Buckingham Pi Theorem and the wind tunnel data confirmed the initial lift calculations of the Flying Dutchmen. Thus the aerodynamic design of the wing was fully justified and incorporated into the final plane design

5 Final Design

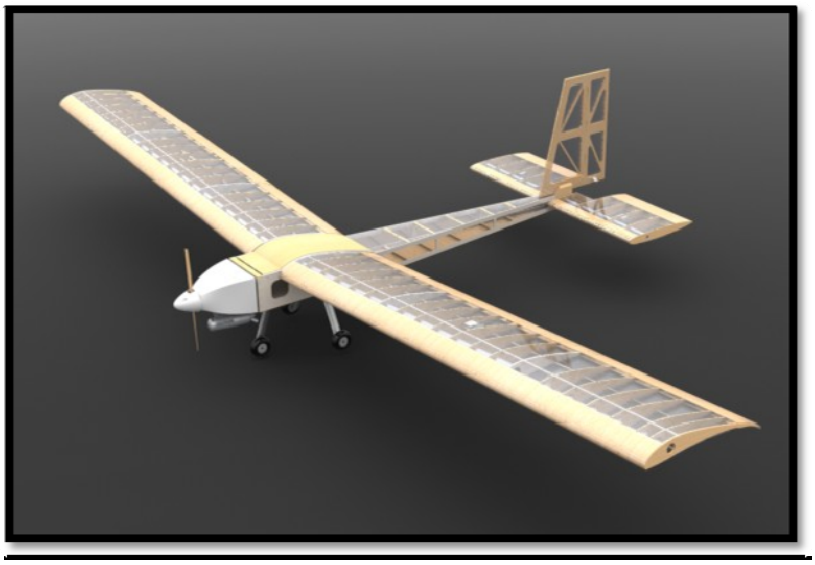

Figure 12*:* Trimetric View of Final Plane Design

Several design trade-offs were considered throughout the construction of the Flying Dutchmen plane. Ultimately, the final plane was built to incorporate a high-wing monoplane design. The planform for the 2011 Dutchmen wing was chosen to be a rectangular. While the chosen planform offered less efficiency than an elliptical design, the constant chord ensured a predictable stall pattern. The Flying Dutchmen also attempted design the planform of the wing to minimize induced drag, which for low-speed flight, is the largest component of plane's overall drag. This goal was achieved by designing a plane with a high aspect ratio and consistent airfoil shape atop the top surface of the fuselage.

One of the later trade-off design decisions made by the 2011 Dutchmen was the conclusion to utilize a tri-gear landing system as opposed to a tail dragger. In reviewing the benefits and pitfalls of each system, the Dutchmen considered the terrain of the

runway, the plane's center of gravity and the overall sizing constraints of the competition. Ultimately, the team made collective decision to utilize the tri-gear system in an attempted to maintain simplistic design and avoid "over engineering" the plane. This mentality reduced the difficulty of construction and helped secure satisfactory results.

The nose cone of the plane was manufactured through the rapid prototype process and custom designed to allow a diagonal engine mount. This ensured that the monokoted wing was protected against excess heat. The nose cone attached directly to the firewall which separates the heat of the engine from the fuel in the fuselage. The fuselage of the 2011 Dutchmen plane was also custom designed. Two noteworthy features of the fuselage include the weight saving cut outs of the non-weight bearing walls and the simplistic puzzle piece design. The simplicity of the fuselage design was only enhanced by the speed and accuracy of the laser cutter, which was utilized to manufacture all precision pieces for the plane, tail boom, tail, and fuselage.

The horizontal stabilizer was designed in such a way that the moment due to its lift, either positive or negative, counteracted the pitching moment from the wing and weight of the motor. The 2011 Flying Dutchmen stabilizer utilizes a NACA symmetrical airfoil, and is approximately twenty-two percent of the wing area where the span and chord are thirty-four and eleven inches respectively. Furthermore, all control surfaces were within convention modeling standard, see Heitmann's report.

Ultimately, the design of the plane promises success at the 2011 SAE Aero competition and the three primary goal of design were obtained. Aerodynamic efficiency can be seen throughout the design, the structural integrity of the plane was considered and constructed in order to withstand several times the weight of the plane, and the overall stability of the plane airs on the conservative side and far exceeds past design's considerations.

6 Non-Technical Achievements

Aside from the aforementioned several non-technical goals were achieved. One resource, developed over the course of the project, which should prove extremely helpful for teams in the future, is the itemized budget for this year' design. The budget, *Figure 13,* lists all material, travel, and competition costs. This budget should prove as an

invaluable resource for future teams during the fundraising portion the competition. Especially once club status for the SAE Aero Union team is established, the proposed budget will help to better allocate funding.

Material Needed for One Wing

	Quantity	Price per unit	Total	Total per Student
1/4" X 1/4" X 3' Spruce Spar	8	$1	$8	$2.67
1/8" X 1/8" X 3' Spruce Spar	3	$0.50	$1.50	$0.50
1/4" X 1/4" X 3' Balsa Spar	4	$0.60	$2.40	$0.80
1/16" X 3" X 3' Balsa Sheet	4	$1.50	$6.00	$2.00
Balsa Leading Edge	3	$3.29	$9.87	$3.29
Monokote	2	$16.00	$32.00	$10.67
Aluminum Bar	1	$24.00	$24.00	$8.00
Micro Servo	1	$22.00	$22.00	$7.33
1/8" X 6" X 3' Balsa Ribs	8	$2.50	$20.00	$6.67
Total Cost of One Wing			**$125.77**	**$41.92**

Material Expenditures

Additional 3 Wings	3	$125.77	$377.31	$125.77
3/8" X 4' X 8' Plywood Fuselage Body	1	$25.97	$25.97	$8.66
1' Aluminum Tubing	2	$18.79	$37.58	$12.53
36" X 1/4" X 1" Aluminum Landing Gear	1	$37.00	$37.00	$12.33
1/8" X 6" X 3' Balsa Ribs in Tail	4	$2.50	$10.00	$3.33
Weights				
Rapid Prototpying	19in^3	$15/in^3	$285	$95
Total Materials Cost			$898.63	$299.54

Travel

Driving Cost/Milage	~2060 miles	$0.505/mi	$1,040	$347
Per Diem Travel Rate	4 days/nights	$100 (first 3 nights), $50 for 4th night	$1,050	$350
Total			**$2,090**	**$696.67**

Competition Expenditures

Andrew's Travel	1	$696.67	$696.67	$696.67
Tim's Travel	1	$696.67	$696.67	$696.67
Angela's Travel	1	$696.67	$696.67	$696.67
Uhaul	7 days	$18.95/day	$132.65	$44.22
Student Coverage of Travel Cost	20%		$305	$102
Registration	$600.00		$600.00	$200.00
Total Competition Cost			$2,822.65	$1,411.33

Figure 13: Itemized Budget

Another accomplishment that greatly benefited our design and construction process this year was a network of modeling enthusiast from the local area. The advice gained from members The Flying Knights club was an integral aspect of the construction phase of this project. The members of the Flying Knights proved to be prepared and often times excited to lend a hand whenever possible and expressed interest in the continued mentoring of future Dutchmen teams. These connections are an invaluable resource and the 2011 team recommends maintaining contact with the gentlemen of the Flying Knights for future advice.

7 Conclusions

In conclusion, the 2011 SAE Aero team has met all project goals and design requirements. Both departmental and competition standards were upheld and the team worked as a cooperative group to achieve the common goal. The plane is currently ready for testing and holds great promise for competition in early spring. The aerodynamics of the entire plane was analyzed and the results considered throughout the design process. This consideration, along with the structural and stability analyses of McGovern and Heitmann, respectively will undoubtedly prove to be beneficial as the plane is tested against teams from all over the globe. This project proved to be an excellent learning opportunity and I am proud to have been a part of this team.

8 References

1. "SAE Collegiate Design Series: Aero Design® East." *Student Central*. Web. 18 Nov. 2010. <http://students.sae.org/competitions/aerodesign/east/>.

2. "Lift | Define Lift at Dictionary.com." *Dictionary.com | Find the Meanings and Definitions of Words at Dictionary.com*. Web. 15 Nov. 2010. <http://dictionary.reference.com/browse/lift>.

3. Jh Phillips, By. "Types of Airplane Drag." *HubPages*. Web. 16 Nov. 2010. <http://hubpages.com/hub/Types-of-Airplane-Drag>.

4. Lennon, Andy. *Basics of R/C Model Aircraft Design: Practical Techniques for Building Better Models*. Ridgefield, CT: Air Age, 1996. Print.

5. "Airfoil Investigation Database - Showing S1223." *Airfoil Investigation Database - Welcome*. Web. 16 Nov. 2010. <http://www.worldofkrauss.com/foils/1421>.

6. "Activity: Four Forces of Flight." *FAA: Home*. Web. 17 Nov. 2010. <http://www.faa.gov/education/educator_resources/educators_corner/grades_7_8/four_forces_of_flight/>.

7. "Wing Geometry Definitions." *Re-Living the Wright Way -- NASA*. Web. 16 Nov. 2010. <http://wright.nasa.gov/airplane/geom.html>.

8. "Definition of Dihedral." *Online Dictionary, Language Guide, Foreign Language and Etymology*. Web. 17 Nov. 2010. <http://www.allwords.com/word-dihedral.html>.

9 Acknowledgements

- Flying Knights Aero Club: Provided modeling expertise and flight testing pilots
    - Tom Hick
    - Ralph Deleon
    - Gerry Garing
    - Daryl Hull
- Prof. Hannay and Hannay Reels Inc.: Donation of $250
- Dean Traver and the Engineering Department: $1,500 Sponsorship
- Stan Gorski: Construction advice and manufactured parts using the laser cutter
- Union College Machine Shop: Construction device
- Rhonda Becker: Aided in ordering parts
- IEF Funding
- Wiggly Worms Bait and Tack: Spring scale donation
- Prof. Ramasubramanian and Prof. Bruno: Project advisors

Appendix A: Test Apparatus

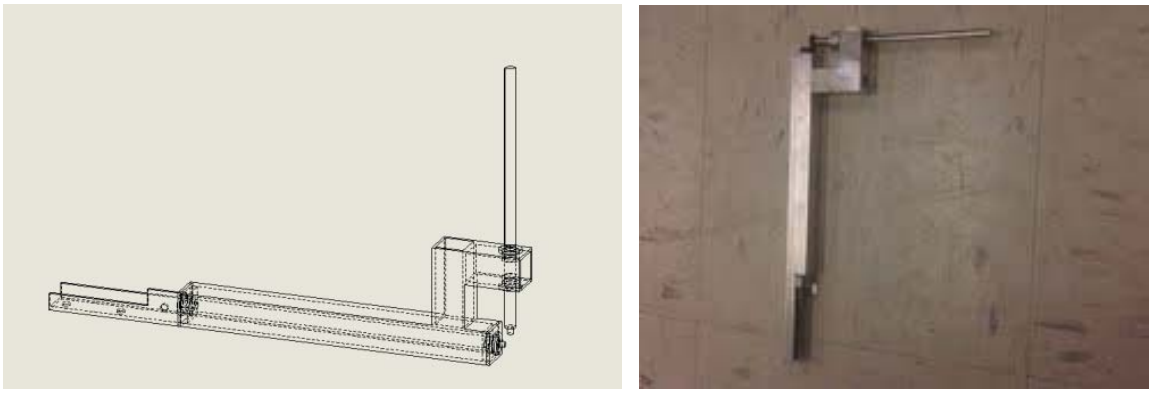

***Figure 14*:** Wind Tunnel, Wing Testing Apparatus

The testing tool shown above will connect to the dynamometer outside the wind tunnel using the screw pattern located towards the bottom of the main shaft. A turn wheel just above this connection point will allow users to alter the angle of the wing while leaving the wind tunnel setup intact.

Appendix B: Payload Prediction Graph

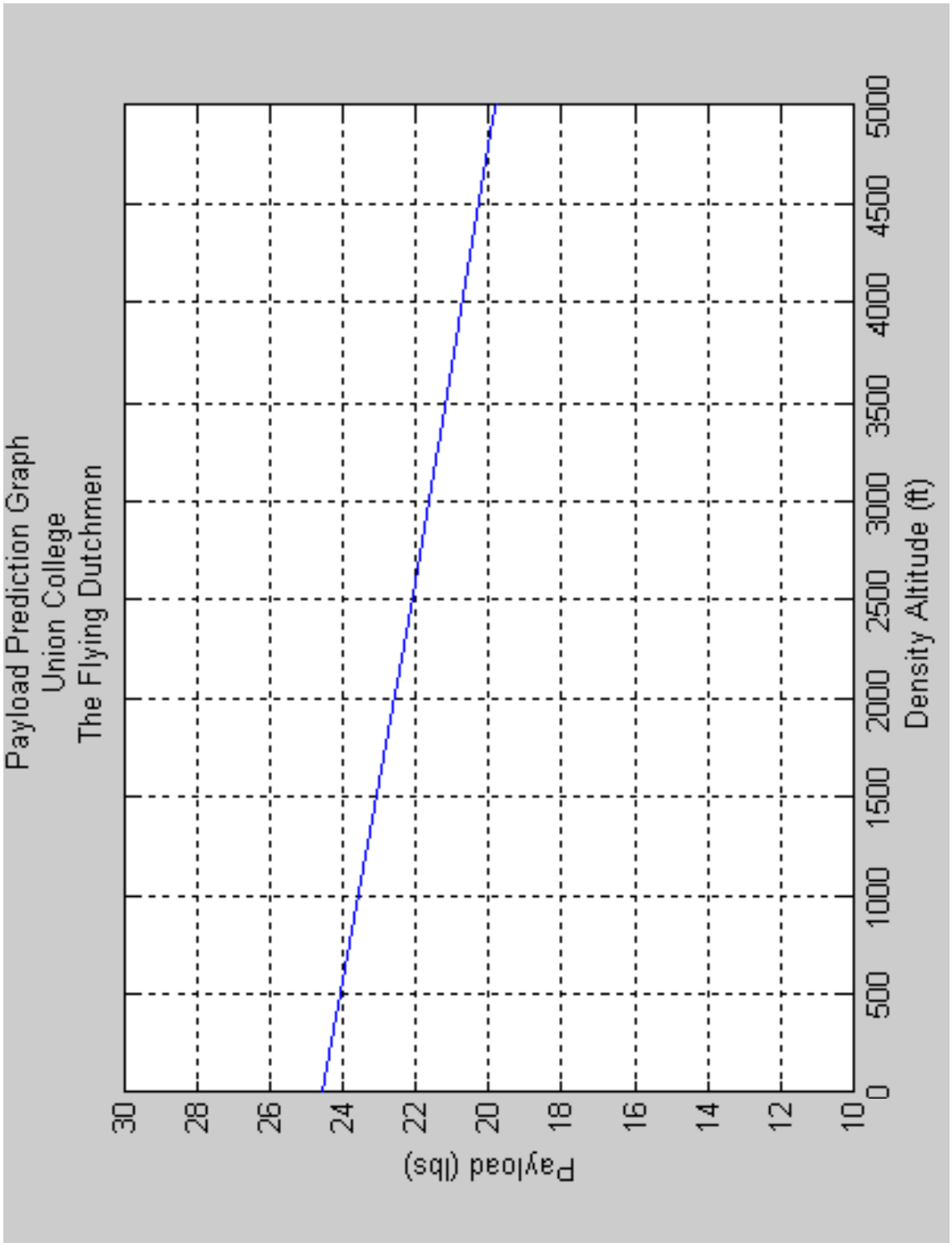

Appendix C: Drawing of Final Plane